Check for updates

Geophysical Research Letters

RESEARCH LETTER
10.1029/2024GL112996

Comparing Estimates of Whitecap Coverage From a Spectral Wave Model With Oceanic Observations

A. H. Callaghan[1], J.-R. Bidlot[2], G. de Leeuw[3,4], and C. D. O'Dowd[5]

[1]Department of Civil and Environmental Engineering, Imperial College London, South Kensington, UK, [2]ECMWF, Reading, UK, [3]Royal Netherlands Meteorological Institute (KNMI), R & D Satellite Observations, De Bilt, The Netherlands, [4]State Environmental Protection Key Laboratory of Satellite Remote Sensing, Aerospace Information Research Institute, Chinese Academy of Sciences, Beijing, China, [5]School of Natural Sciences, Ryan Institute Centre for Climate and Air Pollution Studies, University of Galway, Galway, Ireland

Key Points:

- Values of whitecap coverage made with the ECMWF spectral wave model, ecWAM, are in good agreement with observations from the North Atlantic
- Improved model estimates of W are achieved by introducing a wave age dependency and an energy dissipation rate threshold
- Accurate estimates of whitecap coverage can be made with ecWAM

Supporting Information:

Supporting Information may be found in the online version of this article.

Correspondence to:

A. H. Callaghan,
a.callaghan@imperial.ac.uk

Citation:

Callaghan, A. H., Bidlot, J.-R., de Leeuw, G., & O'Dowd, C. D. (2025). Comparing estimates of whitecap coverage from a spectral wave model with oceanic observations. *Geophysical Research Letters*, *52*, e2024GL112996. https://doi.org/10.1029/2024GL112996

Received 16 OCT 2024
Accepted 14 JAN 2025

Author Contributions:

Conceptualization: A. H. Callaghan
Data curation: A. H. Callaghan
Formal analysis: A. H. Callaghan
Funding acquisition: A. H. Callaghan, G. de Leeuw, C. D. O'Dowd
Investigation: A. H. Callaghan
Methodology: A. H. Callaghan
Resources: G. de Leeuw, C. D. O'Dowd
Validation: A. H. Callaghan
Visualization: A. H. Callaghan
Writing – original draft: A. H. Callaghan
Writing – review & editing: G. de Leeuw, C. D. O'Dowd

© 2025. The Author(s).
This is an open access article under the terms of the Creative Commons Attribution License, which permits use, distribution and reproduction in any medium, provided the original work is properly cited.

Abstract The fractional or percentage whitecap coverage of the ocean surface (W) is often parameterized in terms of wind speed. Data sets of W typically show order of magnitude scatter at a given wind speed value due to sea state variability. Here we compare modeled values of W to measured W values from the North Atlantic Ocean. The modeled W is forced by the spectrally integrated whitecap dissipation source function in the European Center for Medium-Range Weather Forecasts spectral wave model, ecWAM. Without tuning, best agreement is found for mature sea states, with an average modeled to measured W ratio of 0.87. This ratio approaches unity with the introduction of a dissipation rate threshold value and an explicit wave-age dependence. The study suggests that accurate estimates of W can be routinely produced by ecWAM and opens new opportunities to model bubble-mediated fluxes of CO_2 and sea spray aerosol with ecWAM.

Plain Language Summary Predicting the frequency of occurrence and scale of wave breaking at the ocean surface is extremely difficult. In the past, many approaches have used wind speed as a predictor of the ocean surface coverage in whitecap foam (W) generated by sufficiently energetic breaking waves. These relationships do not capture the inherent sea state-dependent variability in wave breaking at a given wind speed and better approaches are needed. In this paper, we show how sophisticated wave models can be used to accurately reproduce measured W values from the North Atlantic over a wind range of wind speeds and sea states. This result implies that we can move away from using wind speed to predict W values. This has positive implications for how bubble-mediated fluxes of greenhouse gases and sea spray aerosol particles can be more accurately parameterized in global climate models.

1. Introduction

When wind-generated surface ocean gravity waves become unstable due to exceeding a kinematic or geometric limiting criterion, or a combination of both, they break and can entrain air beneath the water surface in sufficient volumes to form surface whitecaps. The process of breaking dissipates wave energy and drives a flux of turbulent kinetic energy into the upper ocean (Thomson et al., 2016). The air entrained during the breaking process drives bubble-mediated air-sea exchange processes such as gas transfer (Deike & Melville, 2018; Keeling, 1993; Leighton et al., 2018; Woolf, 1993) and sea spray aerosol production (Blanchard, 1963; De Leeuw et al., 2011; Deike et al., 2022; Monahan et al., 1986) which are fundamental to the evolution of weather and climate. Understanding and modeling breaking waves is an ongoing area of research to help improve the accuracy of spectral wave models and the parameterization of bubble-mediated exchange processes.

Bubble-mediated processes have often been quantified using parameterizations of the sea surface whitecap coverage, W, which are a function of the 10 m neutral wind speed, U_{10N} (e.g., Bell et al., 2017; Callaghan, 2013; Monahan et al., 1986; Woolf, 1993). However, at any given wind speed there exists up to an order of magnitude or more of scatter in values of W highlighting that wind speed alone does not uniquely determine W (Monahan, 1971). Indeed, parameterizations that incorporate sea state development have shown to be as, or more, skillful in constraining variability in W (e.g., Brumer et al., 2017; Zhao & Toba, 2001). Therefore, parameterizations or models of W that can better capture the natural variability in W have the potential to improve how bubble-mediated processes are in turn parameterized.

19448007, 2025, 3, Downloaded from https://agupubs.onlinelibrary.wiley.com/doi/10.1029/2024GL112996 by Imperial College London, Wiley Online Library on [13/05/2025]. See the Terms and Conditions (https://onlinelibrary.wiley.com/terms-and-conditions) on Wiley Online Library for rules of use; OA articles are governed by the applicable Creative Commons License

Breaking waves dissipate wave energy and a link between W and the dissipation rate of turbulent kinetic energy (TKE) per unit sea surface area driven by wave breaking is expected (e.g., Kraan et al., 1996; Ross et al., 1974; Scanlon et al., 2016). Therefore, it is reasonable to assume that a measure of the TKE dissipation rate can provide a suitable variable in place of wind speed alone with which to parameterize W (e.g., Anguelova & Hwang, 2016; Hwang & Sletten, 2008). The aim of this paper is therefore to use the energy dissipation rate-based whitecap coverage model presented in Callaghan (2018) to estimate W and to compare these estimates to the field measurements of W made during the Marine Aerosol Production (MAP) field campaign in the North Atlantic Ocean that were presented in Callaghan et al. (2008). The Callaghan (2018) W model (hereafter referred to as C18) is forced by the spectrally integrated whitecap dissipation source term (ϕ_{oc}) in the European Center for Medium-Range Forecasts (ECMWF) spectral wave model (ecWAM). The ϕ_{oc} values have been interpolated in time and space to match the time and locations of the W measurements. The approach taken here is similar to that of Scanlon et al. (2016) who compared in situ measurements of whitecap coverage to whitecap coverage estimates derived from the model described in Kraan et al. (1996). The current study uses the C18 W model which is based on the experimentally validated model of Callaghan et al. (2016) while the Kraan et al. (1996) model was derived based on the assumption that the wave field energy dissipation rate scales as the product of the wave variance and peak frequency.

Within the broader aim described above, the study provides the opportunity to (a) evaluate the accuracy of the C18 W model to capture the measured variability in W and (b) to understand if the magnitude of ϕ_{oc} in ecWAM is able to reproduce W estimates of comparable magnitude to the oceanic W measurements. The former is important because it provides an opportunity to evaluate the C18 W model using data sets that were not used in its derivation (Callaghan et al., 2012, 2013, 2016; Scanlon & Ward, 2016). The latter is important because it is, in part, the difference between the wind input and dissipation source terms in spectral wave models that drives variability in the modeled energy of a sea state as opposed to the absolute magnitude of the source terms. Indeed, the magnitude of the dissipation term in spectral wave models has been used as a tuning knob and altered to reduce any systematic wave height bias (e.g., Alday & Ardhuin, 2023). Therefore, predictions of W based on ϕ_{oc} provide a useful means to evaluate the magnitude of the spectrally integrated dissipation source term.

The paper proceeds as follows. Section 2 describes the measured W data set, the ECMWF spectral wave model and the C18 W model. Section 3 presents the comparison of modeled and measured W values and evaluates the performance of previous models and parameterizations to predict the measured W data. Finally, our conclusions are presented in Section 4.

2. Methods

2.1. Measured W Data

The W data used here were collected as part of the MAP research cruise that took place in the North Atlantic off the north-west coast of Ireland in 2006. Full details of the image data set, image processing and meteorological conditions are given in Callaghan et al. (2008), and only key details are reproduced here. The W data were generated by applying the Callaghan and White (2009) AWE algorithm to a data set of 43,158 sea surface images collected on seven different days within an 11-day period. The 10-m wind speed varied within the range 4–23 m s^{-1} and young, mature and swell-dominated sea states were sampled. Values of W are typically determined by the rate of air entrainment and subsequent bubble plume degassing in a population of whitecaps as well as surfactant-driven stabilization of surface foam. Ideally, any model estimate of W would include all three processes, but we do not try to estimate the surfactant effect here even though we expect the W measurements to have been influenced to some degree by surfactant-driven foam stabilization.

2.2. The Spectral Wave Model

Model wave data are from a wave hindcast obtained with the ECMWF spectral wave model (ecWAM). It was forced with hourly ERA-5 neutral 10 m winds, air density, wind gustiness and sea ice coverage (Hersbach et al., 2020). We use the hindcast data rather than the ERA5 wave data because the hindcast is based on a more recent version of ecWAM (Cy47r1; ECMWF (2020)), with the improved wave physics for wind input and wave breaking dissipation of Ardhuin et al. (2010), a higher horizontal resolution of 18 km (cubic octahedral reduced Gaussian grid with spectral truncation Tco 639) and a finer spectral resolution (36 directions and 36 frequencies)

19448007, 2025, 3, Downloaded from https://agupubs.onlinelibrary.wiley.com/doi/10.1029/2024GL112996 by Imperial College London, Wiley Online Library on [13/05/2025]. See the Terms and Conditions (https://onlinelibrary.wiley.com/terms-and-conditions) on Wiley Online Library for rules of use; OA articles are governed by the applicable Creative Commons License

compared to ERA5. It has however not used altimeter data assimilation and was not directly coupled to the other components of the ECMWF Earth System Model. The hindcast data for significant wave height and wave period are generally in good agreement with observations (Lobeto et al., 2024). Figure S1 in Supporting Information S1 also confirms that the surface wind conditions during MAP are well captured by ERA-5 across a range of wind speeds and wave ages. The wave age is calculated as the ratio of the phase speed of the waves at the peak of the wave spectrum, c_p, and $U_{10N,ECMWF}$. The value of c_p is calculated from the linear dispersion relation using the peak wave period, T_p.

Spectral wave models such as ecWAM represent the evolution of the two-dimensional wave spectrum due to different physical processes that are acting on the wave field, such as the momentum transfer from wind to waves (wind input), nonlinear wave-wave interaction and the dissipation of wave energy due to wave breaking. These interactions are represented in terms of source terms. Integrating any of these source terms over the two spectral dimensions (frequency and direction) yields the energy flux related to that process. Besides standard integrated wave parameters, ecWAM also outputs the spectrally integrated dissipation source function $\left(\phi_{oc}\right)$. However, because these output parameters are computed over the full frequency range, it is assumed that for frequencies above those resolved prognostically by the model (see Equation 5.4 in ECMWF (2020)), the spectrum is given by Phillips' power law (decay as frequency to the fifth power). It is therefore assumed that there is a balance between wind input, dissipation and the flux due to nonlinear wave-wave interactions (equilibrium range). In practice this means that all energy and momentum going into the high-frequency range of the spectrum, either by wind input or non-linear transfer, is dissipated, and is therefore directly transferred to the ocean column. This balance is used to compute the high frequency contribution of ϕ_{oc} (see Section 10.5.2 in ECMWF (2020) for more details).

2.3. The C18 *W* Model

The whitecap coverage of the sea surface can be written as the sum of the growth phase component W_{growth} and the decay phase component W_{decay}, following $W = W_{growth} + W_{decay}$. The former represents the contribution from whitecaps during their growth phase when foam area increases while air is being entrained up until they reach their maximum area (see Figures 2(a, b) in Callaghan et al. (2017)). The latter represents the contribution from whitecaps during their decay phase when the area of each whitecap decreases with time. This decay stage is driven primarily by bubble plume degassing and surfactant-driven stabilization of foam.

The C18 whitecap coverage model predicts that W_{growth} is linearly proportional to the rate of energy dissipation per unit sea surface area by whitecaps, S_{wcap}–$\left[W\ m^{-2}\right]$, and inversely proportional to the average bubble plume injection depth of a population of whitecaps, $\hat{z}_p^*$, via:

$$W_{growth} = \frac{S_{wcap}}{\Omega \rho \hat{z}_p^*} \tag{1}$$

where ρ is the water density and Ω characterizes the space and time averaged dissipation rate of turbulent kinetic energy inside the bubble plume during active air entrainment with a value of 0.88 $W\ kg^{-1}$. The use of a constant value of Ω comes directly from Figure 2 in Callaghan et al. (2016) and is a manifestation of the fluid turbulence saturation phenomenon described in Deane et al. (2016). Equation 1 can be extended to model W via:

$$W = W_{growth}(1 + \delta) \tag{2}$$

where $\delta = W_{decay}/W_{growth}$. The term δ can be replaced by δ^* which is the component of δ that is driven by bubble plume degassing only and does not account for any surfactant-driven foam stabilization effect. Callaghan (2018) parameterizes δ^* as a function of $\hat{z}_p^*$ forced by the 10-m neutral wind speed. Here, we parameterize $\hat{z}_p^*$ in terms of the significant wave height of the wind waves, $H_{s,ww}$, in order to remove any explicit dependence on $U_{10,N}$ in the C18 W model. The relationship used is given by:

$$\hat{z}_p^* = 0.06(H_{s,ww} - 0.05) + 0.04 \tag{3}$$

19448007, 2025, 3, Downloaded from https://agupubs.onlinelibrary.wiley.com/doi/10.1029/2024GL112996 by Imperial College London, Wiley Online Library on [13/05/2025]. See the Terms and Conditions (https://onlinelibrary.wiley.com/terms-and-conditions) on Wiley Online Library for rules of use; OA articles are governed by the applicable Creative Commons License

where $H_{s,ww}$ is obtained directly from the ecWAM output. A full description of how Equation 3 was obtained is given in Supporting Information S1.

3. Results and Discussion

Having defined the relationship between $\hat{z}_p^*$ and $H_{s,ww}$ with Equation 3, it is now possible to use Equation 2, with δ^* in place of δ, to estimate W with ecWAM. The reason for using δ^* in place of δ is that because while the W measurements likely have some contribution from surfactant-driven foam stabilization, it is not possible to determine this contribution in retrospect. Therefore we choose to use the parameterization for δ^* as described above and in Callaghan (2018). The relation for δ^* is from Equation 21 in Callaghan (2018) and is given as $\delta^* = 8.65\ \hat{z}_p^{*0.69}$. We also use ϕ_{oc} in place of S_{wcap} because while S_{wcap} represents the energy dissipation by whitecaps only, ϕ_{oc} represents the dissipation from all wave processes, but it is not possible to know the proportion of ϕ_{oc} that is driven by whitecaps only (except for depth-induced breaking in very shallow water which is not considered here).

3.1. Initial Results

The first W model we evaluate is given by Equation 4 below and the results are plotted in Figure 1.

$$W = \frac{\phi_{oc}}{\Omega \rho \hat{z}_p^*}(1 + \delta^*) \tag{4}$$

The model W estimates are plotted as a function of wind speed in Figure 1a and compared to the MAP W measurements which are color-coded by wave age as defined in Section 2.2. The $U_{10N,ECMWF}$ is used in place of the measured U_{10} throughout because the ultimate goal is to model W with ecWAM which uses $U_{10N,ECMWF}$. Using measured U_{10} in place of $U_{10N,ECMWF}$ does not change the overall findings presented below. We note that a wave age value of approximately 1.2 corresponds to the value for a mature or fully developed Pierson and Moskowitz spectrum (Holthuijsen, 2007). Following this, and for the purposes of description, we classify sea state as follows: young developing seas have a wave age less than 1, mature or developed seas have a wave age between 1 and 1.2 and old swell-dominated seas have a wave age greater than 1.2.

Figure 1a shows that there is good overlap between modeled and measured W at wind speeds above about 10 $m\ s^{-1}$, which typically correspond to wave age values closer to 1 characteristic of developing and mature sea states, as seen in Figure 1b. At lower wind speeds, the model W estimates lie consistently above the measurements which were evidently made in swell-dominated seas with wave ages largely greater than 1.2.

The measured and modeled W data are plotted as a function of wave age in Figure 1b. As mentioned above, there is good overlap between the two W data sets for sea states with a wave age close to 1. But the modeled W values lie consistently above the measurements for swell-dominated seas. Interestingly, the largest W values for both the measured and modeled W data sets occur in sea states with a wave age close to 1, representing mature sea states which were generally associated with the strongest wind speeds. Moreover, it can be seen from the W measurements, that at a given wave age, W increases with increasing wind speed, which is entirely physically reasonable.

Figures 1c and 1d provide a direct comparison between modeled and measured W. Best agreement occurs for mature seas where it is expected that the rate of energy input to the wave field is balanced by the energy dissipation rate. Indeed, Figures 1c and 1d show that the modeled W values in mature seas lie close to the 1:1 line in comparison to the W measurements and that their ratio exhibits a well-defined peak in the distribution at 1 albeit with an average value of $W_{ECMWF}/W = 0.87$. The comparison suggests that most of the energy dissipated by the wave field is via whitecaps, with contributions from other physical processes being less important. These other physical processes may include shear-driven turbulence (McWilliams et al., 2012), energy dissipation by parasitic capillary waves (Komen et al., 1996), microbreaking (Sutherland & Melville, 2015) and swell dissipation (Ardhuin et al., 2010), as discussed in Thomson et al. (2016) and Callaghan (2020). Given that no model tuning to minimize error between the modeled and measured W datapoints has been undertaken, this result suggests that the magnitudes of (a) the C18 W model relating the rate of energy dissipation to W and (b) the magnitude of ϕ_{oc} in ecWAM, are realistic.

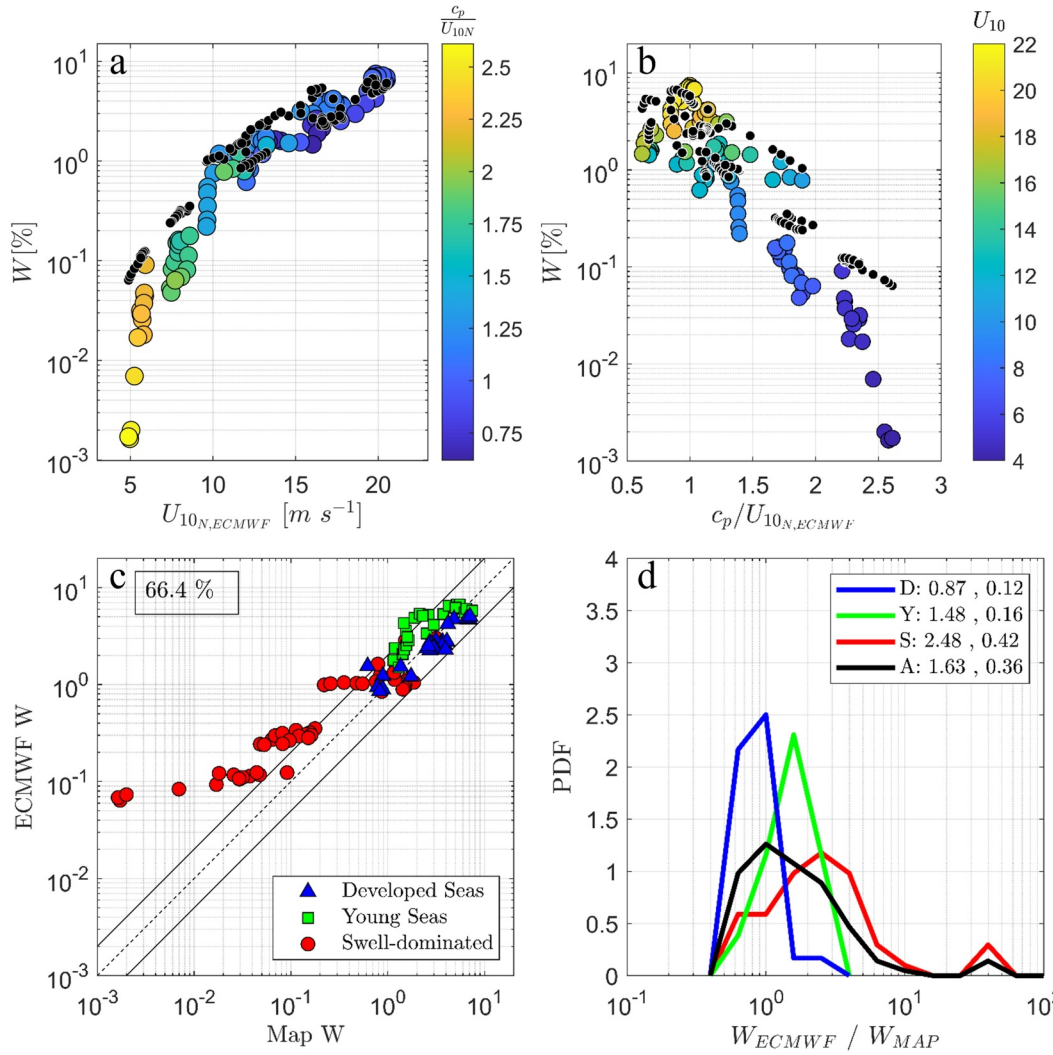


Figure 1. Panel (a) plots the measured (large circles color-coded by wave age) and modeled (black dots) W values as a function of $U_{10N,ECMWF}$ calculated with Equation 4. Panel (b) plots measured (large circles color-coded by $U_{10N,ECMWF}$) and modeled (black dots) W values as a function of wave age. Panel (c) provides a direct comparison between the measured and modeled W values. The color corresponds to wave age values calculated using the phase speed of the peak of the spectrum, c_p, and $U_{10N,ECMWF}$, classified as: Developed Seas ($1 \leq c_p/U_{10,N} \leq 1.2$—blue triangles), Young Seas ($c_p/U_{10,N} < 1.0$—green squares), Swell-dominated Seas ($c_p/U_{10,N} > 1.2$- red circles). The inset number is the % number of modeled W values that lie within a factor of 2 of the W measurements. The dashed line is a 1:1 line. The solid lines lie a factor of 2 above and below the 1:1 line. Panel (d) shows the probability density distributions of the W ratio, separated by the sea state classification (Developed Seas—blue line; Young Seas—green line; Swell-dominated Seas—red line; full data set—black line). The left-hand and right-hand numbers in the legend correspond to the geometric mean and standard deviation of the W ratios for the sea state classifications.

The group of data with the next best level of agreement between measured and modeled W is the young developing sea state group. Here, there is very good agreement in terms of trend between the modeled and measured W datapoints, with the former on average 48% higher than the latter. This overestimation in modeled W may be indicative of the fact that in developing seas, when waves are growing, not all energy input to the wave field is dissipated. Consequently, W modeled with ϕ_{oc} tends to overestimate the measured W values for this sea state classification using Equation 4. While other possibilities relating to inaccuracies in how the wind energy input to the wave field is modulated by a growing sea is represented in the spectral model is possible, it is outside of the scope of this paper to examine this in further detail.

19448007, 2025, 3, Downloaded from https://agupubs.onlinelibrary.wiley.com/doi/10.1029/2024GL112996 by Imperial College London, Wiley Online Library on [13/05/2025]. See the Terms and Conditions (https://onlinelibrary.wiley.com/terms-and-conditions) on Wiley Online Library for rules of use; OA articles are governed by the applicable Creative Commons License

19448007, 2025, 3, Downloaded from https://agupubs.onlinelibrary.wiley.com/doi/10.1029/2024GL112996 by Imperial College London, Wiley Online Library on [13/05/2025]. See the Terms and Conditions (https://onlinelibrary.wiley.com/terms-and-conditions) on Wiley Online Library for rules of use; OA articles are governed by the applicable Creative Commons License

The worst agreement between modeled and measured W occurs in swell-dominated seas and W model estimates are almost 2.5 times larger than the W measurements, on average. The disagreement is most severe at the lowest wind speeds. This suggests that at lower wind speeds, in swell-dominated seas, physical processes that dissipate wave energy but do not manifest as whitecaps play an increasingly important role in the overall balance between wind input and dissipation and whitecapping becomes a secondary process, as noted above. Of these background dissipation processes, only swell dissipation is calculated explicitly in ecWAM.

3.2. Refining the C18 W Model

Having (a) evaluated the C18 W model using ϕ_{oc}, (b) compared the W model estimates to the W measurements and (c) discussed possible sources of disagreement between the two data sets, we now try to refine the W model by introducing physically motivated adjustments to achieve better agreement between the two data sets.

The model refinement uses two additional parameters, namely ϕ_{th} and ξ. The former, ϕ_{th}, is simply a threshold dissipation value which marks the minimum dissipation rate at which whitecaps are expected to first appear, similar to what has been used before in studies relating W to both energy dissipation rate and wind speed (e.g., Monahan & O'Muircheartaigh, 1986; Hwang & Sletten, 2008; Scanlon et al., 2016). The latter, ξ, is a simple scaling factor based on wave age implemented as follows. For developing and mature seas (i.e., $c_p/U_{10,N} \leq 1.2$), $\xi = (c_p/U_{10,N})^2$, while for swell-dominated seas ($c_p/U_{10,N} > 1.2$), $\xi = (1.2 \times U_{10,N}/c_p)^2$. In other words, the model W values are scaled by wave age for mature and developing seas and scaled by inverse wave age for swell-dominated seas. The resulting model is given by

$$W = \frac{\left(\xi\phi_{oc} - \phi_{th}\right)}{\Omega\rho\hat{z}_p^*}(1 + \delta^*) \tag{5}$$

In applying Equation 5, the value of ϕ_{th} was determined via a least squares minimization technique which gave a value of $\phi_{th} = 2.7 \times 10^{-3}\ W\ m^{-2}$. This threshold value is smaller than that reported in Hwang and Sletten (2008) and corresponds to a wind speed value of 2.52 m s^{-1} using Equation 23 of Callaghan (2018).

The result of using Equation 5 to estimate W is shown in Figure 2. Equation 5 provides the best agreement between modeled and measured W values for the data set as a function of wind speed and wave age as seen in Figures 2a and 2b, respectively. Indeed, almost 93% of modeled W datapoints lie within a factor of 2 of the W measurements (see Figure 2c). Moreover, the ratio of modeled to measured W for the three sea state classifications all have a distinctive peak at unity with average values lying within a few percent of 1 (see Figure 2d). It is important to note that the only component of Equation 5 that has been tuned with the MAP W data is ϕ_{th}.

The wave age-dependent scaling factor, ξ, essentially modifies the value of ϕ_{oc} as follows. For developing seas, ξ is always lower than 1, meaning that the fraction of ϕ_{oc} that is due to dissipation by whitecaps is smaller than what would be expected in mature seas. For swell-dominated seas, the value of ξ is also always lower than 1, again indicating that the fraction of ϕ_{oc} that is due to dissipation by whitecaps is smaller than what would be expected in mature seas. Both of these adjustments are easy to justify from a physical argument. Indeed, this result mirrors the findings of Stramska and Petelski (2003), Lafon et al. (2007), Sugihara et al. (2007), and Schwendeman and Thomson (2015). The relevant findings of these studies show that, in general, measured values of W were relatively greater in developed seas than when compared to undeveloped or swell-dominated seas.

For mature seas, ξ takes on a value between 1 and 1.44 and thereby results in an effective increase in the value of ϕ_{oc} for those sea states. For reference, the ensemble averaged value of ξ for the current data set for mature sea states is $\xi = 1.19$. Unlike for the developing and swell-dominated sea states this relative increase in ϕ_{oc} is somewhat harder to physically justify and may reflect a disconnect between the unforced nature of the 2-dimensional breaking wave experiments that informed the C18 W model and wind-forced 3-dimensional breaking waves found in the ocean. For instance, Callaghan et al. (2024) note that bubble plume injection depths are expected to be shallower in wind-forced breaking waves compared to un-forced breaking waves. Additionally, or alternatively, the effective amplification of ϕ_{oc} in mature seas may reflect the fact that the measured W values in mature seas, which typically occurred at higher wind speeds in this study, could have included the effects of surfactant-driven foam stabilization leading to larger W values than otherwise expected.

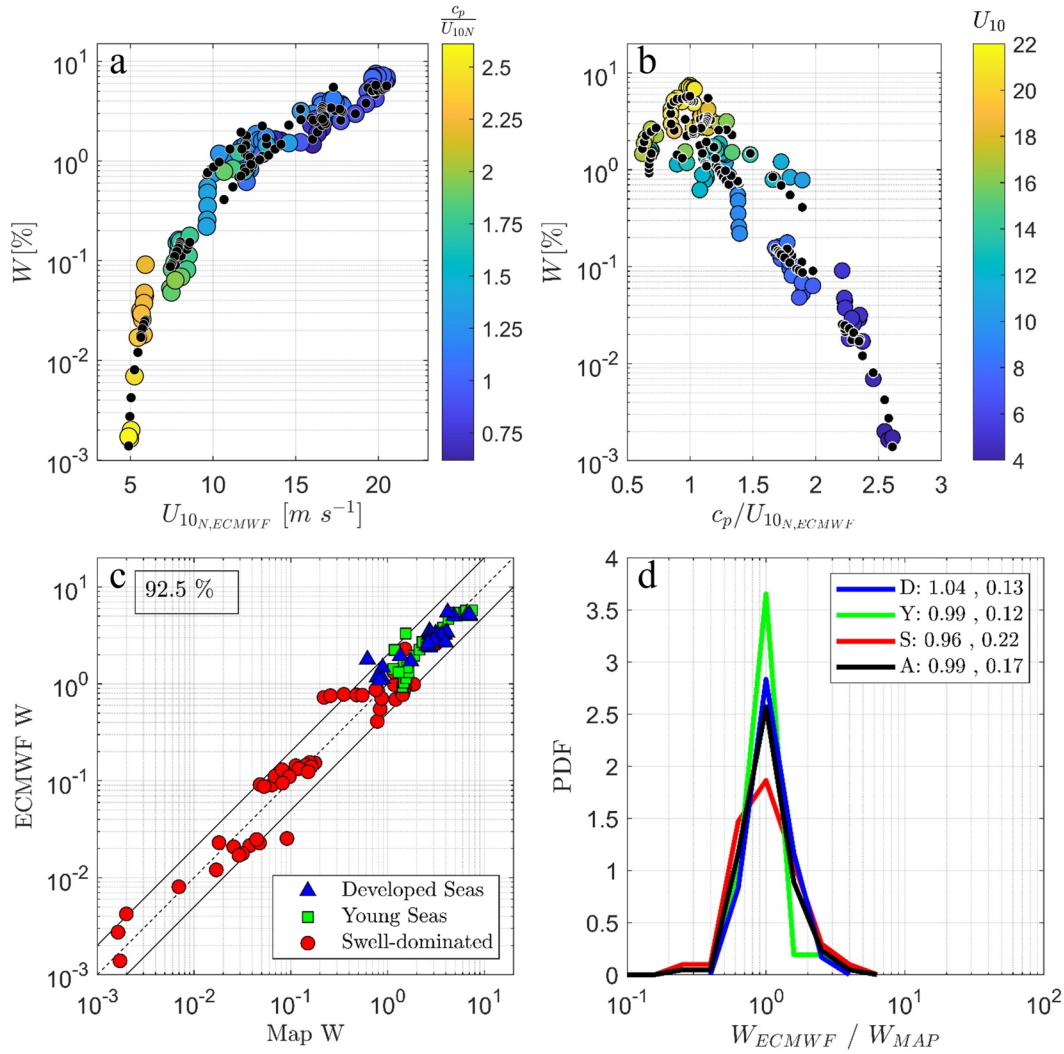


Figure 2. Panel (a) plots the measured (large circles color-coded by wave age) and modeled (black dots) W values as a function of $U_{10N,ECMWF}$ calculated with Equation 5. Panel (b) plots measured (large circles color-coded by $U_{10N,ECMWF}$) and modeled (black dots) W values as a function of wave age. Panel (c) provides a direct comparison between the measured and modeled W values. The inset number is the % number of modeled W values that lie within a factor of 2 of the W measurements. The dashed line is a 1:1 line. The solid lines lie a factor of 2 above and below the 1:1 line. Panel (d) shows the probability density distributions of the W ratio, separated by the sea state classification (Developed Seas—blue line; Young Seas—green line; Swell-dominated Seas—red line; Full data set—black line). The left-hand and right-hand numbers in the legend correspond to the geometric mean and standard deviation of the W ratios for the data sets.

Indeed, previous studies have shown an increase in the contribution to W from stabilized foam with increasing wind speed above about 15 m s^{-1} (Holthuijsen et al., 2012).

As stated above, it has long been held that wave development plays an important role in modulating the degree of whitecapping (e.g., Anguelova & Hwang, 2016; Brumer et al., 2017; Lafon et al., 2004, 2007; Schwendeman et al., 2014; Sugihara et al., 2007; Zhao & Toba, 2001), and this study supports this view quantitatively through the use of wave age is Equation 5. We tested values of ξ that were proportional to wave age, rather than the current quadratic dependence, but this did not work as well. At this stage it is unclear why a quadratic dependence works better than a linear dependence, and understanding why this is should be the focus of further work.

19448007, 2025, 3, Downloaded from https://agupubs.onlinelibrary.wiley.com/doi/10.1029/2024GL112996 by Imperial College London, Wiley Online Library on [13/05/2025]. See the Terms and Conditions (https://onlinelibrary.wiley.com/terms-and-conditions) on Wiley Online Library for rules of use; OA articles are governed by the applicable Creative Commons License

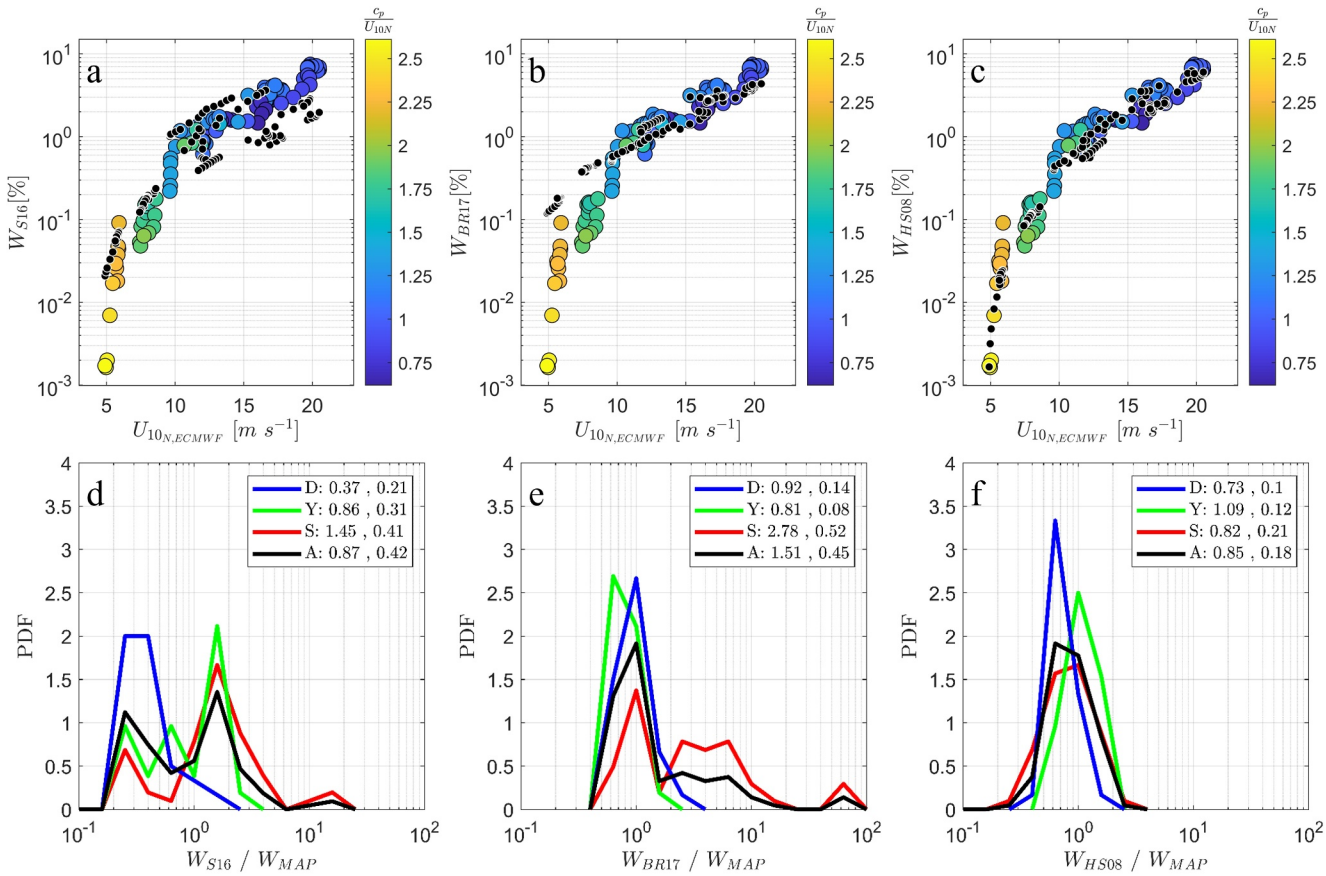


Figure 3. Panels (a–c) show the measured (large circles color-coded by wave age) and modeled (black dots) W values as a function of $U_{10N,ECMWF}$ for the studies of Scanlon et al. (2016), Brumer et al. (2017), and Hwang and Sletten (2008), respectively. Panels (d–f) show the probability density distributions of the ratio of modeled to measured W for the three studies in panels (a–c), respectively. These ratios are separated by the sea state classification (Developed Seas—blue line; Young Seas—green line; Swell-dominated Seas—red line; Full data set—black line). The left-hand and right-hand numbers in the legend correspond to the geometric mean and standard deviation of the W ratios for the three studies.

3.3. Comparison to Previous Studies

We now use the ecWAM data products to evaluate previously published W parameterizations and models and compare their results to the MAP W data set. To do so we use Equation 12 from Scanlon et al. (2016) (S16), the wind-sea wind-wave Reynolds number parameterization from Brumer et al. (2017) (BR17) and the energy-dissipation based model from Hwang and Sletten (2008) (HS08) with their dissipation threshold of $1.3 \times 10^{-2}\ [W\ m^{-2}]$. These parameterizations are given in Section S3 in Supporting Information S1. We note that for the S16 model, we use the mean frequency of the wind sea as recommended in that study.

The results of the comparison between these three studies and the MAP W measurements are presented in Figure 3. The top panels show the estimated W as a function of wind speed plotted with the MAP W measurements. The lower panels show the distribution of the ratio of estimated W to the measured MAP W. It is clear that these three previous studies are able to capture the magnitude and trend of the MAP W data quite well. At wind speeds in excess of 10 m s^{-1}, of these three studies the MAP W values are well represented by both BR17 and HS08. Indeed, the peak of the distribution of W ratios for developed seas lies at unity for BR17, with an average value of 0.92, while HS08 performs best for developing seas. For wind speeds below 10 m s^{-1}, the HS08 model performs best which is helped by the implementation of an energy dissipation threshold.

The rms errors between estimated W and measured W are 0.43, 0.37, and 0.19, for S16, BR17, and HS08 respectively. For comparison, the equivalent rms error for the data in Figure 2 is 0.17, indicating that the current model outperforms S16, BR17, and HS08. Of these three studies investigated here, HS08 performs the best as quantified by the rms error and the shape of the distributions shown in Figure 3f. In conclusion, while none of the

19448007, 2025, 3, Downloaded from https://agupubs.onlinelibrary.wiley.com/doi/10.1029/2024GL112996 by Imperial College London, Wiley Online Library on [13/05/2025]. See the Terms and Conditions (https://onlinelibrary.wiley.com/terms-and-conditions) on Wiley Online Library for rules of use; OA articles are governed by the applicable Creative Commons License

19448007, 2025, 3, Downloaded from https://agupubs.onlinelibrary.wiley.com/doi/10.1029/2024GL112996 by Imperial College London, Wiley Online Library on [13/05/2025]. See the Terms and Conditions (https://onlinelibrary.wiley.com/terms-and-conditions) on Wiley Online Library for rules of use; OA articles are governed by the applicable Creative Commons License

three previous parameterizations perform better than the current ecWAM-C18 W model, the Hwang and Sletten (2008) study shows a comparable level of performance.

4. Summary and Conclusions

We have used the whitecap coverage model of C18, in conjunction with the integrated wave breaking dissipation source term of the ECMWF spectral wave model, ecWAM, to provide estimates of W that are spatially and temporally coincident with W measurements made during the MAP campaign in the North Atlantic Ocean. The W measurements were collected in a range of wind speeds from about 4 $m\ s^{-1}$ to 23 $m\ s^{-1}$ covering young developing seas, mature developed seas and old swell-dominated seas, thereby providing a valuable range of wind and wave conditions. For the purposes of this comparison, we have assumed that the MAP W measurements do not have any contribution from foam patches stabilized by naturally occurring surfactants, but acknowledge that this is almost certainly an oversimplification.

Without tuning, the combined ecWAM-C18 W model performance is best for developed or mature seas. For these sea states, the average value of model to measured W values lies near unity at $W_{ECMWF}/W = 0.87$. The implication is that (a) in mature seas most of the energy dissipated by the wave field is via air-entraining whitecaps and (b) the magnitude of the C18 W model forced with ϕ_{oc} is at a realistic level. We found that the values of W_{ECMWF}/W were typically larger than unity for young, developing seas and old, swell-dominated seas at low wind speeds. A possible explanation for this is that other dissipative mechanisms that do not produce whitecaps are increasingly important in these conditions, as has been postulated in previous studies and described above.

Improved agreement between the modeled and measured W values was achieved by introducing (a) a dissipation threshold (ϕ_{th}) below which whitecaps are not expected and (b) a wave age dependent scaling factor. Doing so provided average W_{ECMWF}/W values within a few percent of unity for the entire data set, along with a reduction in data scatter. Importantly, the only tuning factor we used in this refined model to minimize the root mean square error between modeled and measured W values was ϕ_{th}.

This study demonstrates that ecWAM can be used to generate realistic estimates of W that agree well with in situ measurements from open ocean conditions in the North Atlantic Ocean at large fetch. Consequently, this provides new opportunities for bubble-mediated fluxes of CO_2 and size-resolved sea spray aerosol particles to be estimated with ecWAM using existing W-based parameterizations.

As highlighted by one of the reviewers, more comparisons between measured W data sets and modeled W values would help to establish the broader applicability of the results presented here to other geographical locations and should be the focus of further work. In addition, future work dedicated to comparing W estimates from this model and the work of Romero (2019) which uses the Lambda distribution to estimate W would also be beneficial. Finally we acknowledge that the parameterization used to estimate the bubble plume injection depth during breaking (Equation 3) has not been validated in the field. To do so would need dedicated studies similar to that of Derakhti et al. (2024) and Czerski et al. (2022a, 2022b) but where bubble measurements are concentrated in the upper tens of centimeters or so of the water column which is not at all trivial.

Data Availability Statement

The data presented herein have been uploaded to figshare.com available via Callaghan et al. (2025) at https://doi.org/10.6084/m9.figshare.25460128.v1. For the purpose of open access, the author has applied a Creative Commons Attribution (CC BY) licence to any Author Accepted Manuscript version arising.

Acknowledgments
This work has been funded by the UK Natural Environment Research Council [Grant NE/T000309/1] awarded to AHC. The W data used were collected as part of the Marine Aerosol Production (MAP) project. MAP was financially supported by the European Commission (FP6, project 018332) and participating institutes. We would like to thank Leo Cohen for his crucial role in collecting the digital images of the sea surface that were analysed for whitecap coverage in the MAP campaign.

References

Alday, M., & Ardhuin, F. (2023). On consistent parameterizations for both dominant wind-waves and spectral tail directionality. *Journal of Geophysical Research: Oceans*, *128*(4), 1–21. https://doi.org/10.1029/2022JC019581

Anguelova, M. D., & Hwang, P. A. (2016). Using energy dissipation rate to obtain active whitecap fraction. *Journal of Physical Oceanography*, *46*(2), 461–481. https://doi.org/10.1175/JPO-D-15-0069.1

Ardhuin, F., Rogers, E., Babanin, A., Filipot, J. F., Magne, R., Roland, A., et al. (2010). Semiempirical dissipation source functions for ocean waves. Part I: Definition, calibration, and validation. *Journal of Physical Oceanography*, *40*(9), 1917–1941. https://doi.org/10.1175/2010JPO4324.1

Bell, T. G., Landwehr, S., Miller, S. D., De Bruyn, W. J., Callaghan, A. H., Scanlon, B., et al. (2017). Estimation of bubble-mediated air-sea gas exchange from concurrent DMS and CO_2 transfer velocities at intermediate-high wind speeds. *Atmospheric Chemistry and Physics*, *17*(14), 9019–9033. https://doi.org/10.5194/acp-17-9019-2017

Blanchard, D. C. (1963). The electrification of the atmosphere by particles from bubbles in the sea. *Progress in Oceanography*, *1*(C), 73–202. https://doi.org/10.1016/0079-6611(63)90004-1

Brumer, S. E., Zappa, C. J., Brooks, I. M., Tamura, H., Brown, S. M., Blomquist, B. W., et al. (2017). Whitecap coverage dependence on wind and wave statistics as observed during SO GasEx and HiWinGS. *Journal of Physical Oceanography*, *47*(9), 2211–2235. https://doi.org/10.1175/JPO-D-17-0005.1

Callaghan, A. H. (2013). An improved whitecap timescale for sea spray aerosol production flux modeling using the discrete whitecap method. *Journal of Geophysical Research: Atmospheres*, *118*(17), 9997–10010. https://doi.org/10.1002/jgrd.50768

Callaghan, A. H. (2018). On the relationship between the energy dissipation rate of surface-breaking waves and oceanic whitecap coverage. *Journal of Physical Oceanography*, *48*(11), 2609–2626. https://doi.org/10.1175/JPO-D-17-0124.1

Callaghan, A. H. (2020). Estimates of wave breaking energy dissipation rate from measurements of whitecap coverage. In *Recent advances in the study of oceanic whitecaps* (pp. 25–41). Springer International Publishing. https://doi.org/10.1007/978-3-030-36371-0_3

Callaghan, A. H., Bidlot, J.-R., de Leeuw, G., & O'Dowd, C. (2025). Comparing estimates of whitecap coverage from a spectral wave model with oceanic observations [Dataset]. https://doi.org/10.6084/m9.figshare.25460128.v1

Callaghan, A. H., Deane, G. B., & Stokes, M. D. (2013). Two regimes of laboratory whitecap foam decay: Bubble-plume controlled and surfactant stabilized. *Journal of Physical Oceanography*, *43*(6), 1114–1126. https://doi.org/10.1175/JPO-D-12-0148.1

Callaghan, A. H., Deane, G. B., & Stokes, M. D. (2016). Laboratory air-entraining breaking waves: Imaging visible foam signatures to estimate energy dissipation. *Geophysical Research Letters*, *43*(21), 11320–11328. https://doi.org/10.1002/2016GL071226

Callaghan, A. H., Deane, G. B., & Stokes, M. D. (2017). On the imprint of surfactant-driven stabilization of laboratory breaking wave foam with comparison to oceanic whitecaps. *Journal of Geophysical Research: Oceans*, *122*(8), 6110–6128. https://doi.org/10.1002/2017JC012809

Callaghan, A. H., Deane, G. B., & Stokes, M. D. (2024). A comparison of laboratory and field measurements of whitecap foam evolution from breaking waves. *Journal of Geophysical Research: Oceans*, *129*, 1–18. https://doi.org/10.1029/2023JC020193

Callaghan, A. H., Deane, G. B., Stokes, M. D., & Ward, B. (2012). Observed variation in the decay time of oceanic whitecap foam. *Journal of Geophysical Research*, *117*(9), 1–20. https://doi.org/10.1029/2012JC008147

Callaghan, A. H., de Leeuw, G., Cohen, L., & O'Dowd, C. D. (2008). Relationship of oceanic whitecap coverage to wind speed and wind history. *Geophysical Research Letters*, *35*(23), L23609. https://doi.org/10.1029/2008GL036165

Callaghan, A. H., & White, M. (2009). Automated processing of sea surface images for the determination of whitecap coverage. *Journal of Atmospheric and Oceanic Technology*, *26*(2), 383–394. https://doi.org/10.1175/2008JTECHO634.1

Czerski, H., Brooks, I. M., Gunn, S., Pascal, R., Matei, A., & Blomquist, B. (2022a). Ocean bubbles under high wind conditions—Part 1: Bubble distribution and development. *Ocean Science*, *18*(3), 565–586. https://doi.org/10.5194/os-18-565-2022

Czerski, H., Brooks, I. M., Gunn, S., Pascal, R., Matei, A., & Blomquist, B. (2022b). Ocean bubbles under high wind conditions—Part 2: Bubble size distributions and implications for models of bubble dynamics. *Ocean Science*, *18*(3), 587–608. https://doi.org/10.5194/os-18-587-2022

Deane, G. B., Stokes, M. D., & Callaghan, A. H. (2016). The saturation of fluid turbulence in breaking laboratory waves and implications for whitecaps. *Journal of Physical Oceanography*, *46*(3), 975–992. https://doi.org/10.1175/JPO-D-14-0187.1

Deike, L., & Melville, W. K. (2018). Gas transfer by breaking waves. *Geophysical Research Letters*, *45*(19), 10482–10492. https://doi.org/10.1029/2018GL078758

Deike, L., Reichl, B. G., & Paulot, F. (2022). A mechanistic sea spray generation function based on the sea state and the physics of bubble bursting. *AGU Advances*, *3*(6), 1–19. https://doi.org/10.1029/2022AV000750

De Leeuw, G., Andreas, E. L., Anguelova, M. D., Fairall, C. W., Lewis, E. R., O'Dowd, C., et al. (2011). Production flux of sea spray aerosol. *Reviews of Geophysics*, *49*(2), 1–39. https://doi.org/10.1029/2010RG000349

Derakhti, M., Thomson, J., Bassett, C., Malila, M., & Kirby, J. T. (2024). Statistics of bubble plumes generated by breaking surface waves. *Journal of Geophysical Research: Oceans*, *129*(5), e2023JC019753. https://doi.org/10.1029/2023JC019753

ECMWF. (2020). Part VII: ECMWF wave model IFS DOCUMENTATION—Cy47r1 Operational implementation 30 June 2020 PART VII: ECMWF WAVE MODEL (pp. 1–114). Author. https://doi.org/10.21957/31drbygag

Hersbach, H., Bell, B., Berrisford, P., Hirahara, S., Horányi, A., Muñoz-Sabater, J., et al. (2020). The ERA5 global reanalysis. *Quarterly Journal of the Royal Meteorological Society*, *146*(730), 1999–2049. https://doi.org/10.1002/qj.3803

Holthuijsen, L. H. (2007). *Waves in oceanic and coastal waters*. Cambridge University Press. https://doi.org/10.2277/0521860288

Holthuijsen, L. H., Powell, M. D., & Pietrzak, J. D. (2012). Wind and waves in extreme hurricanes. *Journal of Geophysical Research*, *117*(9), 1–15. https://doi.org/10.1029/2012JC007983

Hwang, P. A., & Sletten, M. A. (2008). Energy dissipation of wind-generated waves and whitecap coverage. *Journal of Geophysical Research*, *113*(2), 1–12. https://doi.org/10.1029/2007JC004277

Keeling, R. F. (1993). On the role of large bubbles in air-sea gas exchange and supersaturation in the ocean. *Journal of Marine Research*, *51*(2), 237–271. https://doi.org/10.1357/0022240933223800

Komen, G. J., Cavaleri, L., Donelan, M., Hasselmann, K., Hasselmann, S., & Janssen, P. (1996). Dynamics and modelling of ocean waves.

Kraan, G., Oost, W. A., & Janssen, P. A. E. M. (1996). Wave energy dissipation by whitecaps. *Journal of Atmospheric and Oceanic Technology*, *13*(1), 262–267. https://doi.org/10.1175/1520-0426(1996)013⟨0262:WEDBW⟩2.0.CO;2

Lafon, C., Piazzola, J., Forget, P., & Despiau, S. (2007). Whitecap coverage in coastal environment for steady and unsteady wave field conditions. *Journal of Marine Systems*, *66*(1–4), 38–46. https://doi.org/10.1016/j.jmarsys.2006.02.013

Lafon, C., Piazzola, J., Forget, P., Le Calve, O., & Despiau, S. (2004). Analysis of the variations of the whitecap fraction as measured in a coastal zone. *Boundary-Layer Meteorology*, *111*(2), 339–360. https://doi.org/10.1023/B:BOUN.0000016490.83880.63

Leighton, T. G., Coles, D. G., Srokosz, M., White, P. R., & Woolf, D. K. (2018). Asymmetric transfer of CO_2 across a broken sea surface. *Scientific Reports*, *8*(1), 1–9. https://doi.org/10.1038/s41598-018-25818-6

Lobeto, H., Semedo, A., Lemos, G., Dastgheib, A., Menendez, M., Ranasinghe, R., & Bidlot, J.-R. (2024). Global coastal wave storminess. *Scientific Reports*, *14*(1), 3726. https://doi.org/10.1038/s41598-024-51420-0

McWilliams, J. C., Huckle, E., Liang, J. H., & Sullivan, P. P. (2012). The wavy Ekman layer: Langmuir circulations, breaking waves, and Reynolds stress. *Journal of Physical Oceanography*, *42*(11), 1793–1816. https://doi.org/10.1175/JPO-D-12-07.1

Monahan, E. C. (1971). Oceanic whitecaps. *Journal of Physical Oceanography*, *1*(2), 2–144. https://doi.org/10.1175/1520-0485(1971)001⟨0139:ow⟩2.0.co;2

Monahan, E. C., & O'Muircheartaigh, I. G. (1986). Whitecaps and the passive remote sensing of the ocean surface. *International Journal of Remote Sensing*, *7*(5), 627–642. https://doi.org/10.1080/01431168608954716

Monahan, E. C., Spiel, D. E., & Davidson, K. L. (1986). Model of marine aerosol generation via whitecaps and wave disruption. In *Oceanic whitecaps* (pp. 147–152). https://doi.org/10.1007/978-94-009-4668-2_16

19448007, 2025, 3, Downloaded from https://agupubs.onlinelibrary.wiley.com/doi/10.1029/2024GL112996 by Imperial College London, Wiley Online Library on [13/05/2025]. See the Terms and Conditions (https://onlinelibrary.wiley.com/terms-and-conditions) on Wiley Online Library for rules of use; OA articles are governed by the applicable Creative Commons License

Romero, L. (2019). Distribution of surface wave breaking fronts. *Geophysical Research Letters*, *46*(17–18), 10463–10474. https://doi.org/10.1029/2019GL083408

Ross, B., Oceanic, N., Oceanographic, A., & Laboratories, M. (1974). Measurements of surface wind speed. *Journal of Geophysical Research*, *79*(3), 444–452. https://doi.org/10.1029/jc079i003p00444

Scanlon, B., Breivik, Ø., Bidlot, J.-R., Janssen, P. A., Callaghan, A. H., & Ward, B. (2016). Modeling whitecap fraction with a wave model. *Journal of Physical Oceanography*, *46*(3), 887–894. https://doi.org/10.1175/JPO-D-15-0158.1

Scanlon, B., & Ward, B. (2016). The influence of environmental parameters on active and maturing oceanic whitecaps. *Journal of Geophysical Research: Oceans*, *121*(5), 3325–3336. https://doi.org/10.1002/2015JC011230

Schwendeman, M., & Thomson, J. (2015). Observations of whitecap coverage and the relation to wind stress, wave slope, and turbulent dissipation. *Journal of Geophysical Research: Oceans*, *120*(12), 8346–8363. https://doi.org/10.1002/2015JC011196

Schwendeman, M., Thomson, J., & Gemmrich, J. R. (2014). Wave breaking dissipation in a young wind sea. *Journal of Physical Oceanography*, *44*(1), 104–127. https://doi.org/10.1175/JPO-D-12-0237.1

Stramska, M., & Petelski, T. (2003). Observations of oceanic whitecaps in the north polar waters of the Atlantic. *Journal of Geophysical Research*, *108*(3), 1–10. https://doi.org/10.1029/2002jc001321

Sugihara, Y., Tsumori, H., Ohga, T., Yoshioka, H., & Serizawa, S. (2007). Variation of whitecap coverage with wave-field conditions. *Journal of Marine Systems*, *66*(1–4), 47–60. https://doi.org/10.1016/j.jmarsys.2006.01.014

Sutherland, P., & Melville, W. (2015). Field measurements of surface and near-surface turbulence in the presence of breaking waves. *Journal of Physical Oceanography*, *45*(4), 943–965. https://doi.org/10.1175/JPO-D-14-0133.1

Thomson, J., Schwendeman, M. S., Zippel, S. F., Moghimi, S., Gemmrich, J. R., & Rogers, W. E. (2016). Wave-breaking turbulence in the ocean surface layer. *Journal of Physical Oceanography*, *46*(6), 1857–1870. https://doi.org/10.1175/JPO-D-15-0130.1

Woolf, D. K. (1993). Bubbles and the air-sea transfer velocity of gases. *Atmosphere-Ocean*, *31*(4), 517–540. https://doi.org/10.1080/07055900.1993.9649484

Zhao, D., & Toba, Y. (2001). Dependence of whitecap coverage on wind and wind-wave properties. *Journal of Oceanography*, *57*(5), 603–616. https://doi.org/10.1023/A:1021215904955

19448007, 2025, 3, Downloaded from https://agupubs.onlinelibrary.wiley.com/doi/10.1029/2024GL112996 by Imperial College London, Wiley Online Library on [13/05/2025]. See the Terms and Conditions (https://onlinelibrary.wiley.com/terms-and-conditions) on Wiley Online Library for rules of use; OA articles are governed by the applicable Creative Commons License